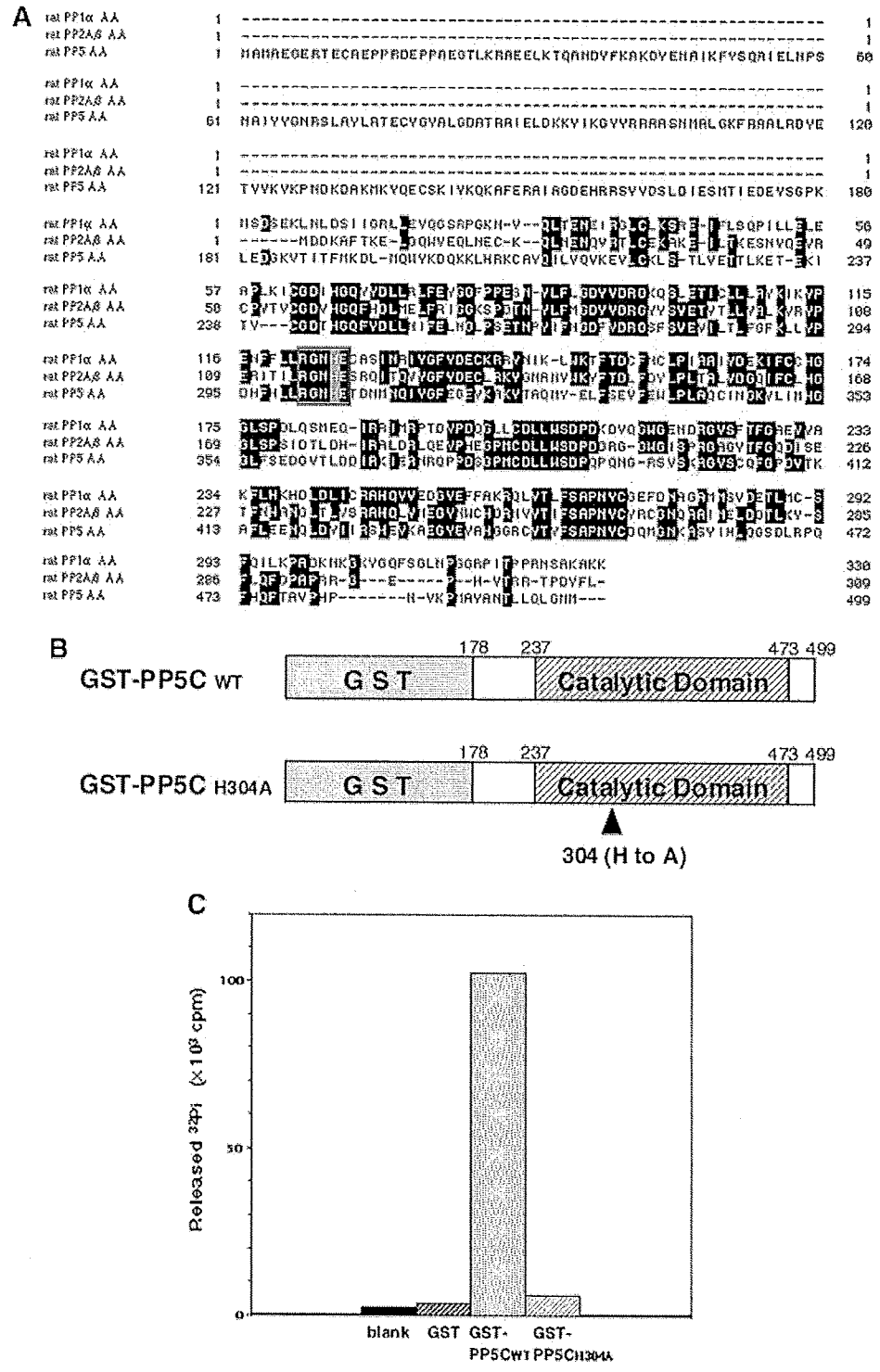

Fig. 1. Generating a phosphatase-dead mutant of PP5. A: Conserved amino acids in the catalytic domain between PP5 and other PPases. Alignment of amino acid sequences of rat PP5, rat PP1α, and rat PP2Aβ. Conserved amino acids are indicated by black shadows. B: Structure of recombinant GST-PP5C expressed in *E. coli*. GST-PP5C$_{WT}$ is a GST-fused PP5 protein, which has the C-terminal catalytic domain of PP5, lacking the N-terminal 177 amino acids. GST-PP5C$_{H304A}$ is a mutant counterpart of GST-PP5$_{WT}$ with an introduced substitution from histidine to alanine at codon 304. C: Phosphatase activities of recombinant GST-PP5C. Phosphatase activities were measured by released ^{32}P using ^{32}P-labeled phospholyrase *a* as a substrate.

and tyrosin at codon 323, is highly conserved among other members of protein phosphatases, such as PP1α and PP2Aβ (Fig. 1A). A single amino acid substitution from histidine to alanine at codon 304 was introduced into GST-$PP5C_{WT}$, aiming to generate a phosphatase-dead mutant of PP5, since amino acid substitution at the corresponding residues of PP1 was reported to lose phosphatase activity [Egloff et al., 1997]. The purified mutant protein, GST-$PP5C_{H304A}$, completely lost phosphorylase *a* phosphatase activity (Fig. 1C). Two other mutant proteins having an amino acid substitution, GST-$PP5C_{D274V}$ and GST-$PP5C_{Y313N}$, lost phosphorylase *a* phosphatase activity as well (data not shown).

Next, we constructed mammalian expression vectors for the full-length rat PP5 fused with EGFP (EGFP-$PP5_{WT}$) and its phosphatase-dead mutant EGFP-$PP5_{H304A}$. Likewise, we also constructed expression vectors for EGFP-$PP5C_{WT}$ and EGFP-$PP5C_{H304A}$, lacking 236 amino acids of the N-terminal part of PP5 (Fig. 2A). After we confirmed that HeLa cells transfected transiently with the plasmids expressed EGFP-$PP5_{WT}$ and EGFP-$PP5_{H304A}$, respectively (data not shown), we attempted to produce tet-on HeLa cells where EGFP-$PP5_{WT}$ or EGFP-$PP5_{H304A}$ was expressed under the control of Dox in the culture medium. Induction of the proteins with Dox was confirmed by immunoprecipitation with anti-GFP antibody (Fig. 2B), followed by immunoblotting with anti-PP5 antibody (data not shown). Immunoprecipitate with anti-GFP antibody from the cells expressing EGFP-$PP5_{WT}$ showed phosphatase activity (Fig. 2C). On the other hand, that from the control cells expressing EGFP alone did not show significant phosphatase activity. The activity of EGFP-$PP5_{WT}$ was remarkably stimulated by arachidonic acid at 160 μM and inhibited by okadaic acid at 100 nM (Fig. 2C). These results indicate that the phosphatase activity monitored in the present study was indeed derived from EGFP-$PP5_{WT}$, not from other phosphatases contaminated in the immunoprecipitate. It was also confirmed that the imunoprecipitate from the cells expressing EGFP-$PP5_{H304A}$ did not show phosphatase activity, even with addition of arachidonic acid (Fig. 2C).

Subcellular Localization of Wild-Type and Phosphatase-Dead Mutant of PP5 in HeLa Cells

When the wild-type PP5 was expressed transiently in HeLa cells as a form of EGFP-$PP5_{WT}$,

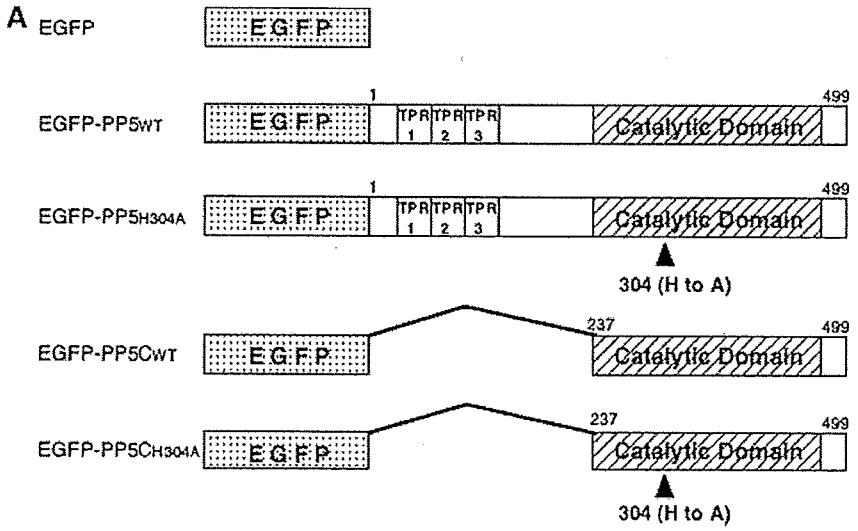

Fig. 2. Establishment of tet-on HeLa cells expressing PP5 or phosphatase-dead mutant. A: Structure of various constructs of EGFP-PP5 for eukaryotic expression. B: Dox-induced expression of EGFP-PP5 proteins in tet-on HeLa cells. A silver-stained SDS–PAGE gel showing immunoprecipitants with anti-GFP antibody from tet-on Hela cells expressing EGFP (**lane 1**), EGFP-$PP5_{WT}$ (**lane 3**), and EGFP-$PP5_{H304A}$ (**lane 5**) in the presence of Dox. Positions of EGFP-PP5s and EGFP are indicated by arrow-heads. C: Phosphatase activities of immunoprecipitants with anti-GFP antibody from each tet-on HeLa cells. Phosphatase activities were measured using *p*-nitrophenylphosphate (PNPP) as a substrate with or without 160 μM of arachidonic acid (AA) and 100 nM of okadaic acid (OA). Open, closed, dotted, and hatched bars indicate (AA+, OA+), (AA+, OA−), (AA−, OA+), and (AA−, OA−), respectively.

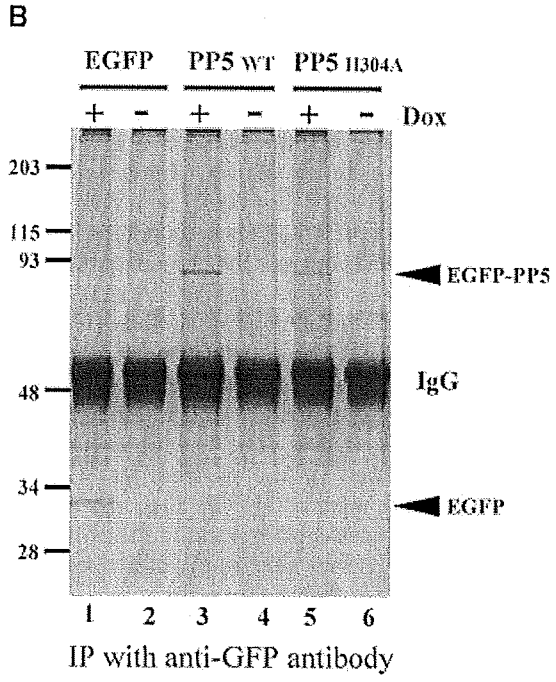

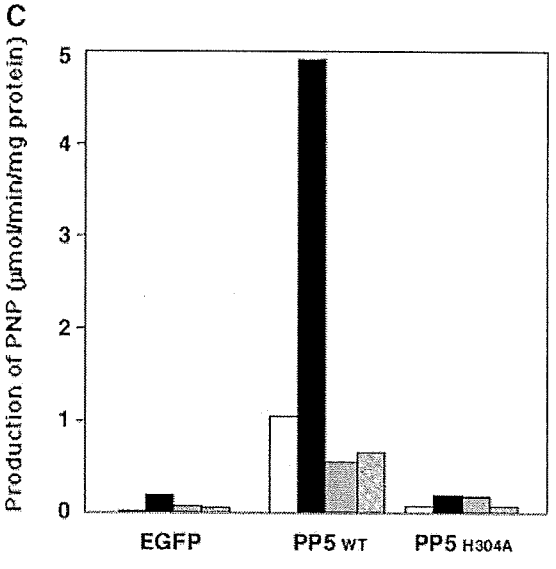

Fig. 2. (*Continued*)

it mainly localized in the cytoplasm and partly at the nucleus (Fig. 3A-c). EGFP-PP5C_{WT}, lacking an N-terminal region, showed a diffused subcellular localization pattern and a considerable fraction of the protein localized in the nucleus, compared to its full-length counterpart, EGFP-PP5$_{WT}$ (Fig. 3A-a). This suggests that TPR motifs in the N-terminal region are necessary for precise localization of PP5 to cytoplasm. No obvious difference was observed in the localization of PP5 between the wild-type and mutant proteins, whether TPR existed (Fig. 3A-c,d) or not (Fig. 3A-a,b).

Induction of Abnormal Nuclear Shape by Transient Expression of PP5 and its Derivatives

Notably, multiple nuclei were frequently observed in HeLa cells transiently trasfected with EGFP-PP5$_{WT}$ at an incidence of more than 20% (Fig. 3B-a). Ratios of cells with deformed nuclear shape were counted and are listed in Table I. HeLa cells transfected with EGFP-PP5$_{WT}$ had deformed nuclei with a 10-fold frequency compared with the control of EGFP. Similarly, the deformed nuclei were induced by the mutant EGFP-PP5$_{H304A}$ with a 10-fold higher frequency compared with the control EGFP (Fig. 3B-c, Table I). Frequencies of deformed nuclei induced by transfection with EGFP-PP5C_{WT} and EGFP-PP5C_{H304A} were increased 2.8- and 3.5-fold compared with EGFP, respectively. These results indicate that the catalytic domain of PP5 does not play an essential role in producing the deformed nuclei, but the N-terminal domain, possibly TPR domains, may contribute to the phenotype.

It is also important to note that the pattern of nuclear shape abnormality was apparently different between the wild-type EGFP-PP5$_{WT}$ and the mutant. EGFP-PP5$_{H304A}$ induced deformed nuclei, which appeared as clover-like segmented shapes having a constricted part (Fig. 3B-c). In contrast, overexpression of wild-type PP5 induced multiple nuclei, each of which seemed to be separated individually by nuclear membrane (Fig. 3B-a). The results suggest the presence of two distinct modes of action for PP5 in the induction of abnormal nuclear shape.

Nuclear Shape Abnormality in *tet-on* HeLa Cells of PP5

To confirm the substantial impact of PP5 on the induction of nuclear shape abnormality, we established several tet-on HeLa cell clones with moderate expression levels of PP5. Induction and activity of the proteins were confirmed by conducting immunoprecipitation and immunoblot analysis as described above. We next examined the effects of PP5-overexpression on nuclear shape using *tet-on* HeLa cells. Induction of EGFP-PP5$_{WT}$ by addition of Dox produced deformed nuclei with a twofold frequency

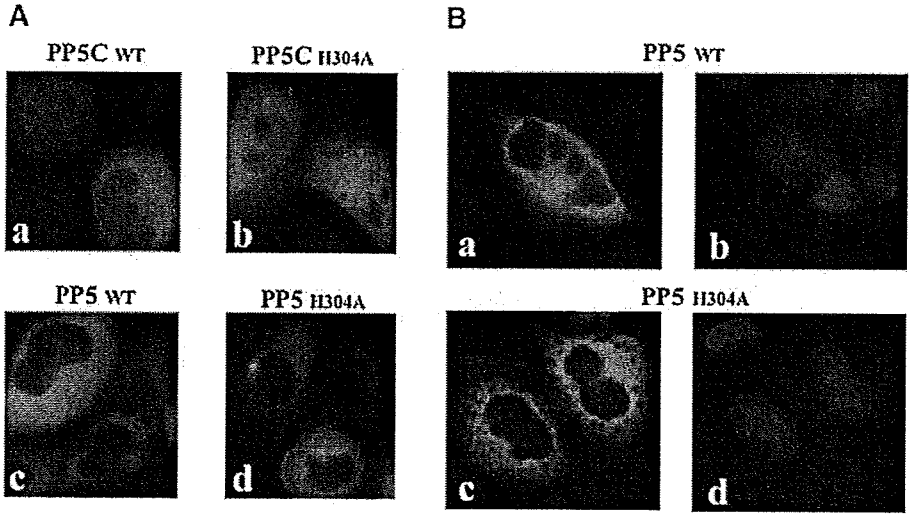

Fig. 3. HeLa cells transfected transiently with EGFP-PP5 variants. A: Fluorescence microscope images of EGFP in the cell expressing EGFP-PP5C_{WT} (a), EGFP-PP5C_{H304A} (b), EGFP-PP5$_{WT}$ (c), and EGFP-PP5$_{H304A}$ (d), showing subcellular localization of each EGFP-PP5 variants. B: Deformed nuclei induced by overexpression of EGFP-PP5 and phosphatase-dead mutants in HeLa cells. Direct fluorescence microscope images of EGFP in the cell expressing EGFP-PP5$_{WT}$ (a) and EGFP-PP5$_{H304A}$ (c), and Hoechst 33342 staining of the same cells (b, d).

as EGFP (Table II). The induction of EGFP-PP5$_{H304A}$ also produced deformed nuclei with a similar frequency to that of EGFP-PP5$_{WT}$ (Table II). Differences between the abnormal nuclear structures induced by the wild-type and mutant PP5 in tet-on HeLa cells were similar to that in transient expressing cells (Fig. 4A). In order to distinguish subtle but distinct differences of the abnormal nuclear structures, lamins A/C and B, backing-up proteins of nuclear membrane, were immunostained (Fig. 4B). Interestingly, *tet-on* HeLa cells expressing EGFP-PP5$_{H304A}$ had deformed nuclei delineated with a continuously reconstructed nuclear membrane (Fig. 4B-c). On the other hand, nuclear membranes were discontinuously formed with the expression of EGFP-PP5$_{WT}$, and deformed nuclei were separated and demarcated individually by nuclear membrane (Fig. 4B-a).

TABLE I. Ratios of Cells With Deformed Nuclei (Transient Transfection)

	Counted cells	No. of cells with deformed nuclei (%)
EGFP-PP5$_{WT}$	379	79 (20.8)
EGFP-PP5$_{H304A}$	299	75 (25.1)
EGFP-PP5C$_{WT}$	319	18 (5.6)
EGFP-PP5C$_{H304A}$	393	28 (7.1)
EGFP	408	8 (2.0)

DISCUSSION

In the present study, we found a novel biological function of PP5 on the reconstruction of nuclear membrane, and a clearly different phenotype was observed between the wild-type and phosphatase-dead mutant PP5. The results embrace two distinct modes of action of PP5: abnormality in nuclear shape was caused in a phosphatase activity-independent manner, but in the N-terminal domain-, possibly a TPR-domain-dependent manner. The results from the inducible expression of PP5 derivatives using *tet-on* HeLa system were in good agreement with those obtained from the transient expression experiment, although the frequencies of the deformed nuclei were lower than that of the transient transfection. The low frequency of abnormal nuclei in tet-on HeLa cells may reflect the expression levels of exogeneously introduced PP5-derivatives per cell, those being

TABLE II. Ratios of Cells With Deformed Nuclei (*Tet-on* HeLa)

	Counted cells	No. of cells with deformed nuclei (%)
EGFP-PP5$_{WT}$	400	52 (13.0)
EGFP-PP5$_{H304A}$	403	57 (14.0)
EGFP	400	28 (7.0)

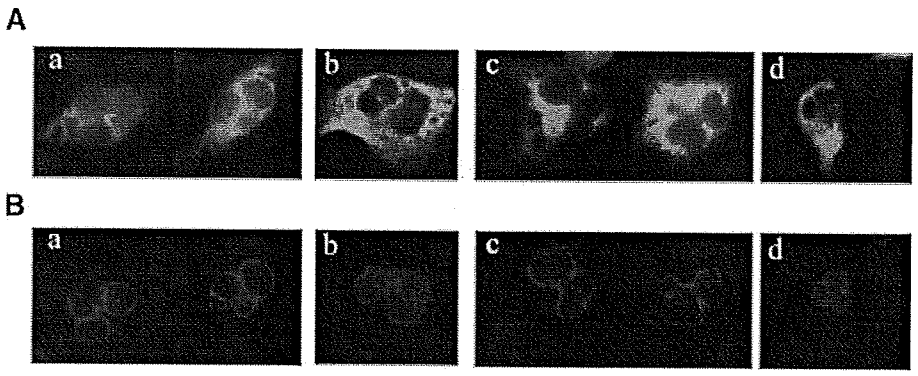

Fig. 4. Differences between the abnormal nuclear structures induced by wild-type and mutant PP5. A: Fluorescence microscope images of EGFP in the tet-on HeLa cells expressing EGFP-$PP5_{WT}$ (**a**, **b**) and EGFP-$PP5_{H304A}$ (**c**, **d**). **B**: Immunostaining with anti-lamin B (**a**, **c**) and anti-lamin A/C (**b**, **d**) antibodies of the same cells as in the upper panel A.

much lower in the inducible system compared to the transient expression system.

In the cases of the transient transfection with EGFP-$PP5C_{WT}$ and EGFP-$PP5C_{H304A}$, which are lacking the N-terminal part containing TPR motifs, the frequency of the deformed nuclei was less than one-third of that with their full-length counterparts. This result indicates the N-terminal domain of PP5 may have a substantial impact on the induction of the deformed nuclei. It is conceivable that the N-terminal domains of EGFP-$PP5_{WT}$ and EGFP-$PP5_{H304A}$ sequester some PP5-associating proteins and a consequent loss of their function may lead to the generation of the deformed nuclei. There are several possible mechanisms for the deformed and multiple nuclei induced by overexpression of EGFP-$PP5_{WT}$ and EGFP-$PP5_{H304A}$, in addition to the absorption of PP5-associating proteins by the TPRs in the EGFP-PP5 proteins described above. (1) Acceleration of the PP5-driven processes by overexpression of PP5; (2) abnormal dephosphorylation of PP5's substrates or other proteins by overexpression of PP5; (3) dominant negative effect of phosphatase-dead mutant; (4) dominant negative effect by EGFP-fused proteins inhibiting the real *in vivo* ability of PP5.

Accumulating studies have suggested that PP5 could be involved in G1 arrest, apoptosis and DNA-damage responses through regulating the activities of p53, ASK-1 and ATM in response to various stresses [Zuo et al., 1998; Morita et al., 2001; Ali et al., 2004]. In addition, our current study suggests the possible involvement of PP5 in chromosome partition in mitosis. Particularly, the phosphatase activity of PP5 is suspected to be required for the last step of chromosome separation and nuclear membrane. Molecular mechanisms of these complex processes are largely unknown and await further investigation. Therefore, we only propose several possible mechanisms to form the unusual shaped nuclei by aberrant PP5 activity here. In the exit from mitosis and progression of cytokinesis, dephosphorylation of many different cyclin-B-cdk-1 substrates is required for different events, including cytokinesis, spindle disassembly, and nuclear reformation [Pines, 2006]. Nuclear reassembly requires phosphate activity, and at least for B-type lamins, involves PP1 [Steen and Collas, 2001; Margalit et al., 2005]. It is, therefore, highly possible that PP5 is also involved in nuclear reassembly and other events in the late or post-mitotic stages. PP5 was reported to colocalize with both cytoplasmic dynein and microtubles [Galigniana et al., 2002]. Because nuclear envelope breakdown is dynein- and microtubule-dependent [Beaudouin et al., 2002; Salina et al., 2002], it is possible that a dynein- and microtubule-dependent event is also required for nuclear envelope reformation and PP5 modulates this event. Another possibility is abnormality of APC/C function by aberrant PP5 activity may lead to deformed nuclei because PP5 associates with two components of anaphase-promoting complex (APC), CDC16, and CDC27 [Ollendorff and Donoghue, 1997]. PP5 was recently reported to be an inactivator for Raf [von Kriegsheim et al., 2006], and it was reported by many studies that Raf/MEK/ERK signal pathways induced cell

cycle progression via multiple effecter molecules, including p53, p21, p16, and cyclins [Chang et al., 2003]. Therefore, it is possible that misregulation of downstream genes of the Raf pathway induced by aberrant PP5 activity leads to the deformed nuclei.

ACKNOWLEDGMENTS

The study was supported by Grant-in-Aid for Cancer Research from The Ministry of Health, Labour and Welfare of Japan.

REFERENCES

Ali A, Zang J, Bao S, Liu I, Otterness D, Dean NM, Abraham RT, Wang XF. 2004. Requirement of protein phosphatase 5 in DNA-damage-induced ATM activation. Genes Dev 18:249–254.

Beaudouin J, Gerlich D, Daigle N, Eils R, Ellenberg J. 2002. Nuclear envelope breakdown proceeds by microtubule-induced tearing of the lamina. Cell 108:83–96.

Becker W, Kentrup H, Klumpp S, Schultz JE, Joost HG. 1994. Molecular cloning of a protein serine/threonine phosphatase containing a putative regulatory tetratricopeptide repeat domain. J Biol Chem 269:22586–22592.

Chang F, Steelman LS, Shelton JG, Lee JT, Navolanic PM, Blalock W, Franklin R, McCubrey JA. 2003. Regulation of cell cycle progression and apoptosis by the Ras/Raf/MEK/ERK pathway. Int J Oncol 22:469–480.

Chen MX, Cohen PTW. 1997. Activation of protein phosphatase 5 by limited proteolysis or the binding of polyunsaturated fatty acids to the TPR domain. FEBS Lett 400:136–140.

Chen MX, McPartlin AE, Brown L, Chen YH, Barker HM, Cohen PT. 1994. A novel human protein serine/threonine phosphatase, which possesses four tetratricopeptide repeat motifs and localizes to the nucleus. EMBO J 13: 4278–4290.

Chen MS, Silverstein AM, Pratt WB, Chinkers M. 1996. The tetratricopeptide repeat domain of protein phosphatase 5 mediates binding to glucocorticoid receptor heterocomplexes and acts as a dominant negative mutant. J Biol Chem 271:32315–32320.

Chinkers M. 1994. Targeting of a distinctive protein-serine phosphatase to the protein kinase-like domain of the atrial natriuretic peptide receptor. Proc Natl Acad Sci USA 91:11075–11079.

Chinkers M. 2001. Protein phosphatase 5 in signal transduction. Trends Endocrinol Metab 12:28–32.

Cohen PTW. 1997. Novel protein serine/threonine phosphatases: Variety is the spice of life. Trends Biochem Sci 22:245–251.

Egloff MP, Johnson DF, Moorhead G, Cohen PT, Cohen P, Barford D. 1997. Structural basis for the recognition of regulatory subunits by the catalytic subunit of protein phosphatase 1. EMBO J 16:1876–1887.

Fukuda H, Shima H, Vesonder RF, Tokuda H, Nishino H, Katoh S, Tamura S, Sugimura T, Nagao M. 1996. Inhibition of protein serine/threonine phosphatases by fumonisin B1, a mycotoxin. Biochem Biophys Res Commun 220:160–165.

Galingniana MD, Harrell JM, Murphy PJ, Chinkers M, Radanyi C, Renoir JM, Zang M, Pratt WB. 2002. Binding of hsp90-associated immunophilins to cytoplasmic dynein: Direct binding and in vivo evidence that the peptidyl-prolyl isomerase domain is a dynein interaction domain. Biochemistry 41:13602–13610.

Gong CX, Liu F, Wu G, Rossie S, Wegiel J, Li L, Grundke-Iqbal I. 2004. Dephosphorylation of microtubule-associated protein tau by protein phosphatase 5. J Neurochem 88:298–310.

Kang H, Sayner SL, Gross KL, Russell LC, Chinkers M. 2001. Identification of amino acids in the tetratricopeptide repeat and C-terminal domains of protein phosphatase 5 involved in autoinhibition and lipid activation. Biochemistry 40:10485–10490.

Lamb JR, Tugendreich S, Hieter P. 1995. Tetratrico peptide repeat interactions: To TPR or not to TPR? Trends Biochem Sci 20:257–259.

MacKintosh C, Moorhead G. 1993. Assay and purification of protein (serine/threonine) phosphatases. In: Hardie DG, editor. Protein phosphorylation: A practical approach. Oxford: Oxford Univ Press. pp 153–182.

Margalit A, Vlcek S, Gruenbaum Y, Foisner R. 2005. Breaking and making of the nuclear envelope. J Cell Biochem 95:454–465.

Morita K, Saitoh M, Tobiume K, Matsuura H, Enomoto S, Nishitoh H, Ichijo H. 2001. Negative feedback regulation of ASK1 by protein phosphatase 5 (PP5) in response to oxidative stress. EMBO J 20:6028–6036.

Ollendorff V, Donoghue DJ. 1997. The serine/threonine phosphatase PP5 interacts with CDC16 and CDC27, two tetratricopeptide repeat-containing subunits of the anaphase-promoting complex. J Biol Chem 272:32011–32018.

Pines J. 2006. Mitosis: A matter of getting rid of the right protein at the right time. Trends Cell Biol 16:55–63.

Ramsey AJ, Chinkers M. 2002. Identification of potential physiological activators of protein phosphatase 5. Biochemistry 41:5625–5632.

Salina D, Bodoor K, Eckley DM, Schroer TA, Rattner JB, Burke B. 2002. Cytoplasmic dynein as a facilitator of nuclear envelope breakdown. Cell 108:97–107.

Sambrook J, Russel DW. 2001. Molecular cloning: A laboratory manual, 3rd edition. New York: Cold Spring Harbor Laboratory Press. pp 13.7–13.10.

Silverstein AM, Galigniana MD, Chen MS, Owens-Grillo JK, Chinkers M, Pratt WB. 1997. Protein phosphatase 5 is a major component of glucocorticoid receptor-hsp90 complexes with properties of an FK506-binding immunophilin. J Biol Chem 272:16224–16230.

Sinclair C, Borchers C, Parker C, Tomer K, Charbonneau H, Rossie S. 1999. The tetratricopeptide repeat domain and a C-terminal region control the activity of Ser/Thr protein phosphatase 5. J Biol Chem 274:23666–23672.

Skinner J, Sinclair C, Romeo C, Armstrong D, Charbonneau H, Rossie S. 1997. Purification of a fatty acid-stimulated protein-serine/threonine phosphatase from bovine brain and its identification as a homolog of protein phosphatase 5. J Biol Chem 272:22464–22471.

Steen RL, Collas P. 2001. Mistargeting of B-type lamins at the end of mitosis. Implication on cell survival and regulation of lamins a/c expression. J Cell Biol 153:621–626.

von Kriegsheim A, Pitt A, Grindlay GJ, Kolch W, Dhillon AS. 2006. Regulation of the Raf-MEK-ERK pathway by protein phosphatase 5. Nat Cell Biol 8:1011–1016.

Yang J, Roel SM, Cliff MJ, Williams MA, Ladbury JE, Cohen PTW, Barford D. 2005. Molecular basis for TPR domain-mediated regulation of protein phosphatase 5. EMBO J 24:1–10.

Zeke T, Morrice N, Vázquez-Martin C, Cohen PTW. 2005. Human protein phosphatase 5 dissociates from heat-shock proteins and is proteolytically activated in response to arachidonic acid and the microtubule-depolymerizing drug nocodazole. Biochem J 385:45–56.

Zhang J, Bao S, Furumai R, Kucera KS, Ali A, Dean NM, Wang XF. 2005. Protein phosphatase 5 is required for ATR-mediated checkpoint activation. Mol Cell Biol 25: 9910–9919.

Zuo Z, Dean NM, Honkanen RE. 1998. Serine/threonine protein phosphatase type 5 acts upstream of p53 to regulate the induction of p21(WAF1/Cip1) and mediate growth arrest. J Biol Chem 273:12250–12258.

Effect of Running Training on DMH-Induced Aberrant Crypt Foci in Rat Colon

NORIYUKI FUKU[1], MASAKO OCHIAI[2], SHIN TERADA[1], ERI FUJIMOTO[1], HITOSHI NAKAGAMA[2], and IZUMI TABATA[1]

[1]*Division of Health Promotion and Exercise, National Institute of Health and Nutrition, Tokyo, JAPAN; and* [2]*Biochemistry Division, National Cancer Center Research Institute, Tokyo, JAPAN*

ABSTRACT

FUKU, N., M. OCHIAI, S. TERADA, E. FUJIMOTO, H. NAKAGAMA, and I. TABATA. Effect of Running Training on DMH-Induced Aberrant Crypt Foci in Rat Colon. *Med. Sci. Sports Exerc.*,Vol. 39, No. 1, pp. 70–74, 2007. **Purpose:** We examined the effects of treadmill-running training on the induction of aberrant crypt foci (ACF), which is the first step of colon cancer induction, in the colonic mucosa of rats injected with 1,2-dimethylhydrazine (DMH). **Methods:** Four-week-old F344 rats ($N = 38$) were randomly assigned to training (19 rats) and control (19 rats) groups. After a week, all rats were given DMH (20 $mg \cdot kg^{-1}$ body weight) once a week for 2 wk. Running training was started at age 7 wk (speed: 10 $m \cdot min^{-1}$, 0% grade, 120 $min \cdot d^{-1}$, 5 $d \cdot wk^{-1}$). After 4 wk of training, the rats were sacrificed and the colon was removed, opened, and counted for ACF with 0.2% methylene blue staining. **Results:** Running training resulted in lower body- ($P < 0.01$) and adipose fat weight ($P < 0.05$). The numbers of ACF and total AC were significantly lower in the running training group than in the control group ($P < 0.05$). The occurrences of one, three, and five aberrant crypts per focus were also significantly lower in the running training group than in the control group ($P < 0.05$). The ratios of total AC/ACF did not significantly differ between the running training and control groups. **Conclusions:** The results of the present investigation suggest that low-intensity running training inhibits the DMH-induced initiation of colon ACF development. **Key Words:** EXERCISE, ACF, 1,2-DIMETHYLHYDRAZINE, COLON CANCER, PRIMARY PREVENTION, PHYSICAL ACTIVITY

Cancer of the large intestine is classified into colon and rectal cancers. The incidence of colon cancer is increasing at a faster rate than that of rectal cancer in recent years in advanced countries, including Japan. Colon cancers develop after the multistep accumulation of genetic and epigenetic induction of oncogenes in both humans and experimental animals (9,14,19).

The proposed multisteps of colon carcinogenesis may start when aberrant crypt foci (ACF) appear in the colon (37). ACF were defined as lesions composed of enlarged crypts, slightly elevated above the surrounding mucosa and more densely stained with methylene blue than normal crypts (3). ACF are considered to be putative preneoplastic colon lesions that may be early indicators of colon carcinogenesis (4,10,18).

Epidemiological evidence has suggested that physical activity has a protective effect on colon cancer incidence (11,13,30). However, few experimental studies have been conducted to elucidate the mechanisms of exercise-related effects on colon cancer. For example, a few earlier animal studies found that both voluntary (1,26) and treadmill (36) running training reduced tumor incidence after the administration of 1,2-dimethylhydrazine (DMH) or azoxymethane. Furthermore, no studies have examined the effects of physical exercise training on colon cancer as they might be related to the multistep nature of colon carcinogenesis, although Demarzo et al. (7) recently reported that a single session of exhaustive exercise increased the number of ACF DMH-induced rat colons. Up to now, there is no study demonstrating that exercise training affects the number of ACF, which is a putative initial step of colon carcinogenesis of rats. Therefore, we investigated the effects of running exercise training on the number of DMH-induced ACF, because previous studies suggested that physical training of this type has a protective effect on colon tumor incidence in rats.

Address for correspondence: Izumi Tabata, Ph.D., FACSM, Division of Health Promotion and Exercise, Incorporated Administrative Agency National Institute of Health and Nutrition, 1-23-1 Toyama, Shinjuku City, Tokyo, 162-8636, Japan; E-mail: tabata@nih.go.jp.
Submitted for publication March 2006.
Accepted for publication July 2006.

0195-9131/07/3901-0070/0
MEDICINE & SCIENCE IN SPORTS & EXERCISE®

DOI: 10.1249/01.mss.0000239398.78331.96

MATERIALS AND METHODS

Materials

All chemicals, including 1,2-dimethylhydrazine (DMH), a carcinogenic chemical of the colon, was purchased from SIGMA (St. Louis, MO).

Exercise Protocols

Animal care. All experimentation was conducted in accordance with policy statement of the American College of Sports Medicine on research with experimental animals and was approved by the animal care and use committee of National Institute of Health and Nutrition. Four-week-old Fischer 344 male rats were purchased from CLEA Japan, Tokyo. The animals were housed in rooms lighted from 7 a.m. to 7 p.m. and were maintained on an *ad libitum* diet of standard chow and water. The room temperature was maintained at 20–22°C.

Experimental design. After 1 wk of acclimatization to the housing environment (5 wk of age), the rats were randomly assigned to one of two groups: the treadmill-running training group (N = 19) or the control group (N = 19). All rats were given a subcutaneous injection of DMH at a dose level of 20 mg·kg^{-1} body weight, once a week for 2 wk. The DMH was dissolved in 0.1 mM EDTA (pH 6.5) immediately before the administration.

One week after the last injection of DMH (i.e., at age 7 wk), running training was started. The training rats ran for 120 min·d^{-1} (two 60-min bouts separated by 10 min of rest) on a flat motorized treadmill (Natsume, Tokyo, Japan). On the first day, the rats were accustomed to running at a speed of 10 m·min^{-1} by gradually increasing the treadmill speed to the fixed speed. The running speed was maintained for the following 4 wk of training. The intensity of this training was considered to be low because this exercise could be continued for more than 6 h without exhaustion, as reported elsewhere (34).

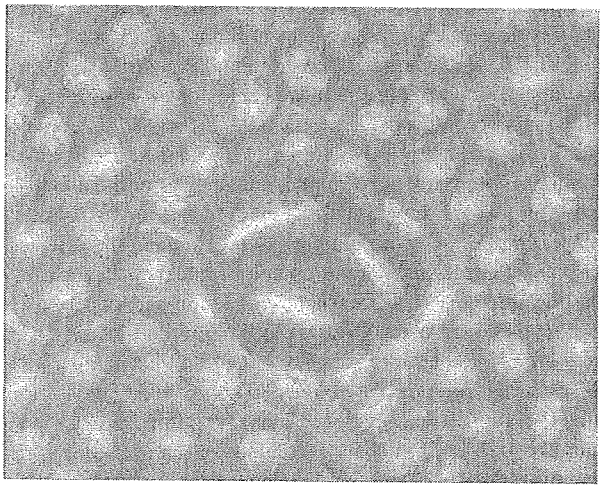

FIGURE 1—1,2-dimethylhydrazine–induced ACF in methylene blue–stained colonic mucosa. In particular, ACF is indicated by the three aberrant crypts per focus that have large crypts, altered luminal openings, and thickened epithelia. This micrograph shows an ACF that consists of three AC. ACF, aberrant crypt foci; AC, aberrant crypts.

TABLE 1. The effect of treadmill-running training on body weight, muscle weight of the heart and soleus, adipose tissue weight of the peritoneum and epididymides, and citrate synthase activity of soleus muscle in rats.

	Control Group (N)	Training Group (N)
BW (g)	216.7 ± 3.5 (19)	199.1 ± 4.0 (19)**
Heart weight (mg·g^{-1} BW)	2.89 ± 0.04 (11)	3.00 ± 0.04 (10)*
Soleus weight (mg·g^{-1} BW)	0.33 ± 0.01 (19)	0.37 ± 0.01 (19)**
Peritoneal adipose tissue weight (mg·g^{-1} BW)	15.0 ± 0.7 (19)	10.2 ± 0.6 (19)***
Epididymides adipose tissue weight (mg·g^{-1} BW)	15.1 ± 0.7 (19)	10.2 ± 0.6 (19)*
Brown adipose tissue weight (mg·g^{-1} BW)	1.50 ± 0.07 (11)	1.28 ± 0.10 (10)
Citrate synthase activity in soleus muscle (μmol·g^{-1} wet tissue·min^{-1})	35.9 ± 1.0 (19)	40.3 ± 1.2 (19)**

Values are means ± SE. BW, body weight. *,**,*** indicate significant differences from the control group at levels of $P < 0.05$, 0.01, and 0.001, respectively, by t-test.

Two or three days after the last bout of exercise, the rats were anesthetized with an intraperitoneal injection of pentobarbital sodium (50 mg·kg^{-1} body weight), and the heart and soleus muscles were excised, weighed, quickly clamp-frozen in liquid nitrogen, and stored at −80°C until analysis. Then, the colons were dissected and gently flushed with 10% neutralized formalin to remove residual bowel contents, cut open longitudinally, fixed flat between filter papers, and submerged in 10% neutralized formalin overnight at 4°C (23). Peritoneal fat, epididymides fat, and brown adipose tissue (BAT) were excised and weighed.

Detection of ACF. Fixed colons were stained with 0.2% methylene blue, as described by Bird (3). The number of ACF and total number of aberrant crypts (AC) comprising ACF were counted for each colon. The ratio of total AC/ACF was calculated to assess ACF multiplicity. As shown in Figure 1, ACF were identified as lesions composed of enlarged crypts, with an increased pericryptal area, a slightly elevated appearance above the surrounding mucosa with an oval or slitlike orifice, and a higher staining intensity with 0.2% methylene blue than normal crypts (3).

Citrate synthase activity in skeletal muscle. Ten percent homogenates were made from the muscle in 175 mM KCl, 10 mM glutathione, and 2 mM EDTA, pH 7.4. The homogenate was frozen and thawed four times and mixed thoroughly before enzymatic measurements. As a maker of oxidative enzyme, citrate synthase (CS) activity in the soleus muscle was measured using Srere's method (31).

Statistical Analysis

All data are shown as the mean ± SE. Quantitative clinical data were compared between run-trained rats and controls by use of the unpaired t-test. ACF-related data were also compared by use of the Mann–Whitney rank sum test because the numbers of ACF were not normally distributed. These data were analyzed by use of SigmaStat for Windows (SPSS Inc., Chicago, IL). Differences were considered significant when the P value was less than 0.05.

RESULTS

Physical characteristics and citrate synthase activity. The body weight of the training rats was

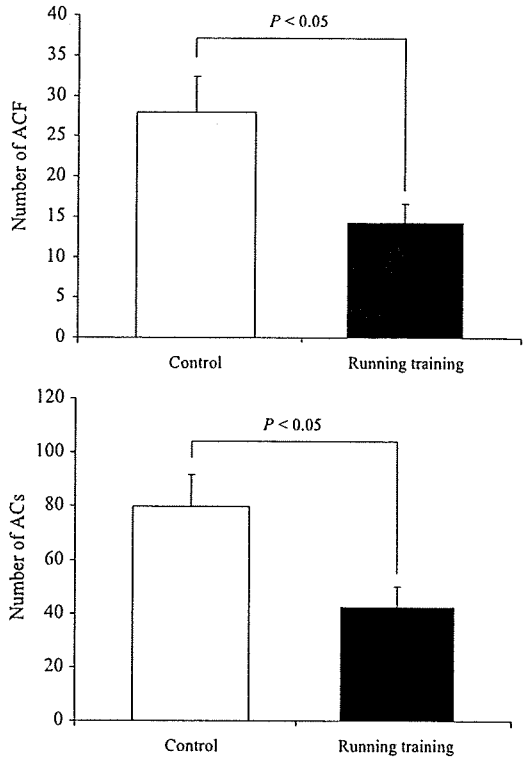

FIGURE 2—Effect of running training on the number of 1,2-dimethylhydrazine-induced ACF (*upper*) and AC (*lower*) in the rat colon. ACF, aberrant crypt foci; AC, aberrant crypts.

significantly less than that of the control rats ($P < 0.01$) (Table 1). The weight of heart and soleus, expressed relative to body weight, was significantly heavier in the training group compared with the control group ($P < 0.05$ and $P < 0.001$, respectively), whereas the relative adipose tissue weight of the peritoneum and epididymides was significantly lighter in the training group compared with the control group ($P < 0.001$ and $P < 0.05$, respectively).

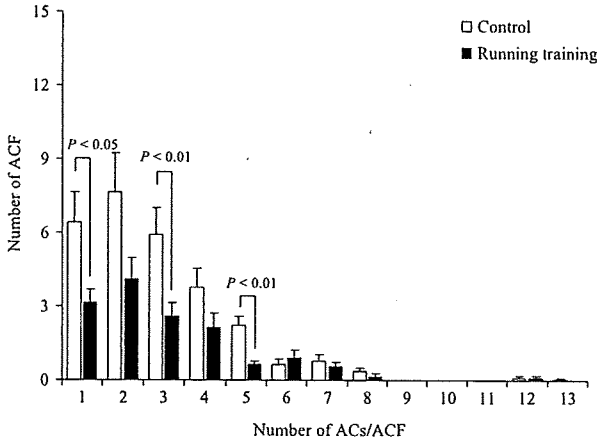

FIGURE 3—Effect of running training on the number of 1,2-dimethylhydrazine-induced AC per focus in the rat colon. ACF, aberrant crypt foci; AC, aberrant crypts.

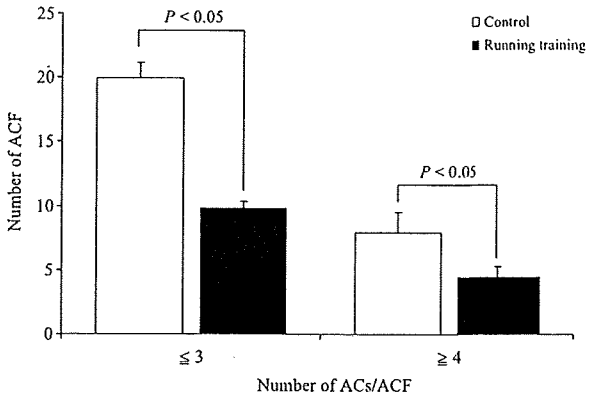

FIGURE 4—Effect of running training on the number of 1,2-dimethylhydrazine-induced small ACF (aberrant crypts per focus ≤ 3) and large ACF (aberrant crypts per focus ≥ 4) in the rat colon. ACF, aberrant crypt foci; AC, aberrant crypts.

The relative BAT weight of the training rats tended to be lower than that of the control group ($P = 0.07$). CS activity in the soleus muscle of the training group was significantly higher than in the control group ($P < 0.05$).

Induction of ACF and AC. As shown in Figure 2 upper panel, the number of ACF of training-group rats was significantly less than that observed in the control group ($P < 0.05$). The number of total AC was also significantly less in the training group than in the control group ($P < 0.05$; Fig. 2 lower panel). As shown in Figure 3, the occurrences of one, three, and five aberrant crypts per focus were significantly smaller in the training group than in the control group ($P < 0.05$). Furthermore, running training decreased the number of not only small ACF, which consists of less than or equal to three AC ($P < 0.05$), but also large ACF (≥ 4 AC) ($P < 0.05$), as compared with the control group (Fig. 4). However, the ratio of total AC/ACF, which indicates the average size of induced ACF, did not significantly differ between the training and control groups (2.9 ± 0.2 vs 2.9 ± 0.7, $P > 0.10$).

DISCUSSION

The main finding of the present study was that short-term, low-intensity running training reduced DMH-induced ACF production in the rat colon.

Colon carcinogenesis is well known to be a multistep process involving multiple genetic alterations (15,37,38). In humans, mutation of adenomatous polyposis coli (APC) gene is regarded as the initial event in ACF, followed by additional mutation of *K-ras* gene in adenomas; further mutation of the *p53* gene is the progressive event in carcinomas (14,33). In rodents, β-catenin mutations are frequently observed in colon tumors and in dysplastic ACF induced by azoxymethane (32). APC and/or K-ras mutations are also occasionally observed in rodents, as they are in humans (32), and ACF has been considered a very initial lesion in a

multistep colorectal tumorigenesis model (14). After ACF were first described in animals, similar lesions were found in humans (28). Because previous studies have suggested that low-intensity, long-term treadmill-running training prevented the incidence or development of colon tumors in a rat model injected subcutaneously with azoxymethane (36), it is reasonable to speculate that exercise training may exert its effect on one or more steps in colon carcinogenesis. To date, however, it remains unknown at which step of the carcinogenic process (e.g., ACF, adenomas (early, intermediate, and late), or carcinomas) physical exercise training exerts its preventive effect in rodents injected with carcinogens. The present results suggest that training in rats suppressed the first step, the initiation of ACF development in the rat colon. This is the first observation regarding the effect of physical exercise on ACF, the development of which is considered the first step in colon carcinogenesis. Furthermore, Colbert et al. (5), using the APC^{Min} mouse model, reported a trend toward fewer polyps in the colon in treadmill-exercised males compared with nonexercised mice. From the present investigation, it is obvious that the earlier phase of colon carcinogenesis is inhibited by exercise training. Therefore, it is of great importance when considering efficient chemopreventive effects on cancer development. Several hypotheses have been suggested to explain the preventive effects of exercise/physical activity on colon carcinogenesis—for example, shortened gastrointestinal transit time as a result of exercise (6); energy balance (16); reduced levels of blood insulin, which might be a growth factor for colon cancer cells (12); enhanced immune activity–related NK cells (20); enhanced free-radical scavenger system (8); changed prostaglandin levels (17); and decreased obesity (25). However, mechanisms related to the exercise-induced decrease in AC and/or ACF are not known at all. Therefore, only a few hypotheses can be raised. First, as Lasko and Bird et al. (16) have reported that caloric restriction–induced weight loss suppressed the increase in the number of ACF after the injection of azoxymethane in rats, it may be possible that energy balance (29), including energy expenditure and reduced food intake (24) or reduced nonexercise activity level (35) by exercise training, may exert a suppressive effect similar to that of caloric restriction, inhibiting the initiation or proliferation of ACF on the colonic mucosa. In fact, the results of the present study indicate that the body weight and/or adipose tissue weight of the peritoneum and epididymides were significantly lower in the running group than in the control group. Therefore, it is plausible that body- or fat weight loss yielded by physical exercise may reduce the initiation of ACF. Another plausible mechanism is that exercise might exhibit its preventive effects on mutation induction in the APC, *K-ras*, and/or *p53* genes through the induction of some detoxification enzymes for oxidative stresses. A third possibility is the commitment of moderate levels of physical exercise on the improvement of lipid metabolism. High fat levels in serum and low expression levels of lipid metabolism–related genes such as lipoprotein lipase in the liver and colon are now considered to have some significant impact on the development of intestinal tumors in the APC^{Min} mouse model (21,22). Further studies are expected to investigate the molecular mechanisms underlying exercise-induced effects on AC/ACF formation.

Recently, Demarzo and Garcia (7) reported that a single bout of exhaustive swimming exercise with a 2% weight tied to the tail was related to an elevated number of colonic ACF in untrained rats treated with DMH, when compared with a control group. Because this report included no description of the exercise protocol, such as a period of acclimatization that is usually given before acute bouts of exercise (27), it is not known how much "stress" was imposed on the exercised rats in the study. Therefore, we could not discuss the different effects of ACF production between the two studies in terms of exercise training–induced stress. On the other hand, the intensity of the swimming exercise with a 2% weight tied to the tail might be higher than that of the running training adopted in the present investigation. Thus, the exercise intensity may be a key factor determining the number of ACF after exercise. In fact, unaccustomed exhaustive and/or high-intensity exercise increases systemic free-radical generation in experimental animals (2). On the other hand, in the present study, we showed that low-intensity physical exercise for 2 h may decrease the development of colonic ACF in experimental animals. Furthermore, stress related to exercise at times during which the rats normally sleep may influence the ACF number in the colon. Therefore, voluntary exercise during the night cycle may be a better alternative exercise protocol than the "forced daytime" treadmill running adopted in the present investigation. However, because the number of ACF in the trained rats in the present study was actually lower than in the nonexercise control group, the overall effects of treadmill running on ACF production are favorable. Therefore, the benefits of the exercise training adopted in the present study are thought to outweigh the disadvantages of exercise-related stress. A future study using voluntary exercise should be conducted to clarify this issue.

The number of AC with a specific number of ACF (1,3,5) in the trained rats was lower than in the control group in the present investigation. However, running training did not affect the overall mean AC/ACF ratios of the rat colon induced by DMH. Thus, it is suggested that the physical exercise training adopted in the present investigation may not be effective for preventing the proliferation of ACF in rat colonic mucosa.

In conclusion, the results of the present investigation demonstrated that low-intensity running training inhibits the initiation of ACF in the rat colon induced by DMH. Furthermore, the present investigation suggests that increasing physical activity might be effective for primary prevention of colon cancer incidence, not only for rats but also for humans, by affecting the first step of cancer induction. However, the clinical implications and pathophysiological mechanisms of these findings warrant further investigation.

This work was supported in part by the Grants-in-Aid for Scientific Research on Exploratory Areas (16650160 to I.T.) from the Ministry of Education, Culture, Sports, Science and Technology, Japan, and by the Sasakawa Scientific Research Grant (to N.F.) from The Japan Science Society. The present addresses of Drs. N. Fuku and S. Terada are Division of Genomics for Longevity and Health, Tokyo Metropolitan Institute of Gerontology, Tokyo, Japan; and Washington University School of Medicine, St. Louis, MO, respectively.

REFERENCES

1. Andrianopoulos, G., R. L. Nelson, C. T. Bombeck, and G. Souza. The influence of physical activity in 1,2 dimethylhydrazine induced colon carcinogenesis in the rat. *Anticancer Res.* 7:849–852, 1987.
2. Banerjee, A. K., A. Mandal, D. Chanda, and S. Chakraborti. Oxidant, antioxidant and physical exercise. *Mol. Cell Biochem.* 253:307–312, 2003.
3. Bird, R. P. Observation and quantification of aberrant crypts in the murine colon treated with a colon carcinogen: preliminary findings. *Cancer Lett.* 37:147–151, 1987.
4. Bird, R. P. Role of aberrant crypt foci in understanding the pathogenesis of colon cancer. *Cancer Lett.* 93:55–71, 1995.
5. Colbert, L. H., J. M. Davis, D. A. Essig, A. Ghaffar, and E. P. Mayer. Exercise and tumor development in a mouse predisposed to multiple intestinal adenomas. *Med. Sci. Sports Exerc.* 32:1704–1708, 2000.
6. Cordain, L., R. W. Latin, and J. J. Behnke. The effects of an aerobic running program on bowel transit time. *J. Sports Med. Phys. Fitness* 26:101–104, 1986.
7. Demarzo, M. M., and S. B. Garcia. Exhaustive physical exercise increases the number of colonic preneoplastic lesions in untrained rats treated with a chemical carcinogen. *Cancer Lett.* 216:31–34, 2004.
8. Duthie, G. G., J. D. Robertson, R. J. Maughan, and P. C. Morrice. Blood antioxidant status and erythrocyte lipid peroxidation following distance running. *Arch. Biochem. Biophys.* 282:78–83, 1990.
9. Esteller, M., P. G. Corn, S. B. Baylin, and J. G. Herman. A gene hypermethylation profile of human cancer. *Cancer Res.* 61:3225–3229, 2001.
10. Fenoglio-Preiser, C. M., and A. Noffsinger. Aberrant crypt foci: a review. *Toxicol. Pathol.* 27:632–642, 1999.
11. Friedenreich, C. M., and M. R. Orenstein. Physical activity and cancer prevention: etiologic evidence and biological mechanisms. *J. Nutr.* 132:3456S–3464S, 2002.
12. Giovannucci, E. Insulin and colon cancer. *Cancer Causes Control* 6:164–179, 1995.
13. Kato, I., S. Tominaga, and A. Ikari. A case-control study of male colorectal cancer in Aichi Prefecture, Japan: with special reference to occupational activity level, drinking habits and family history. *Jpn. J. Cancer Res.* 81:115–121, 1990.
14. Kinzler, K. W., and B. Vogelstein. Lessons from hereditary colorectal cancer. *Cell* 87:159–170, 1996.
15. Kountouras, J., P. Boura, and N. J. Lygidakis. New concepts of molecular biology for colon carcinogenesis. *Hepatogastroenterology* 47:1291–1297, 2000.
16. Lasko, C. M., and R. P. Bird. Modulation of aberrant crypt foci by dietary fat and caloric restriction: the effects of delayed intervention. *Cancer Epidemiol. Biomarkers Prev.* 4:49–55, 1995.
17. Martinez, M. E., D. Heddens, D. L. Earnest, et al. Physical activity, body mass index, and prostaglandin E2 levels in rectal mucosa. *J. Natl. Cancer Inst.* 91:950–953, 1999.
18. McLellan, E. A., A. Medline, and R. P. Bird. Sequential analyses of the growth and morphological characteristics of aberrant crypt foci: putative preneoplastic lesions. *Cancer Res.* 51:5270–5274, 1991.
19. Nagao, M., T. Ushijima, M. Toyota, R. Inoue, and T. Sugimura. Genetic changes induced by heterocyclic amines. *Mutat. Res.* 376:161–167, 1997.
20. Nieman, D. C., S. L. Nehlsen-Cannarella, P. A. Markoff, et al. The effects of moderate exercise training on natural killer cells and acute upper respiratory tract infections. *Int. J. Sports Med.* 11:467–473, 1990.
21. Niho, N., M. Mutoh, M. Takahashi, K. Tsutsumi, T. Sugimura, and K. Wakabayashi. Concurrent suppression of hyperlipidemia and intestinal polyp formation by NO-1886, increasing lipoprotein lipase activity in Min mice. *Proc. Natl. Acad. Sci. USA* 102:2970–2974, 2005.
22. Niho, N., M. Takahashi, T. Kitamura, et al. Concomitant suppression of hyperlipidemia and intestinal polyp formation in Apc-deficient mice by peroxisome proliferator-activated receptor ligands. *Cancer Res.* 63:6090–6095, 2003.
23. Ochiai, M., M. Ushigome, K. Fujiwara, et al. Characterization of dysplastic aberrant crypt foci in the rat colon induced by 2-amino-1-methyl-6-phenylimidazo[4,5-b]pyridine. *Am. J. Pathol.* 163:1607–1614, 2003.
24. Oscai, L. B., and J. O. Holloszy. Effects of weight changes produced by exercise, food restriction, or overeating on body composition. *J. Clin. Invest.* 48:2124–2128, 1969.
25. Parker, E. D., and A. R. Folsom. Intentional weight loss and incidence of obesity-related cancers: the Iowa Women's Health Study. *Int. J. Obes. Relat. Metab. Disord.* 27:1447–1452, 2003.
26. Reddy, B. S., S. Sugie, and A. Lowenfels. Effect of voluntary exercise on azoxymethane-induced colon carcinogenesis in male F344 rats. *Cancer Res.* 48:7079–7081, 1988.
27. Ren, J. M., C. F. Semenkovich, E. A. Gulve, J. Gao, and J. O. Holloszy. Exercise induces rapid increases in GLUT4 expression, glucose transport capacity, and insulin-stimulated glycogen storage in muscle. *J. Biol. Chem.* 269:14396–14401, 1994.
28. Roncucci, L., D. Stamp, A. Medline, J. B. Cullen, and W. R. Bruce. Identification and quantification of aberrant crypt foci and microadenomas in the human colon. *Hum. Pathol.* 22:287–294, 1991.
29. Slattery, M. L., M. Murtaugh, B. Caan, K. N. Ma, S. Neuhausen, and W. Samowitz. Energy balance, insulin-related genes and risk of colon and rectal cancer. *Int. J. Cancer* 115: 148–154, 2005.
30. Slattery, M. L., and J. D. Potter. Physical activity and colon cancer: confounding or interaction? *Med. Sci. Sports Exerc.* 34: 913–919, 2002.
31. Srere, P. Citrate synthase. *Method Enzymol.* 13:3–5, 1969.
32. Takahashi, M., and K. Wakabayashi. Gene mutations and altered gene expression in azoxymethane-induced colon carcinogenesis in rodents. *Cancer Sci.* 95:475–480, 2004.
33. Takayama, T., M. Ohi, T. Hayashi, et al. Analysis of K-ras, APC, and beta-catenin in aberrant crypt foci in sporadic adenoma, cancer, and familial adenomatous polyposis. *Gastroenterology* 121:599–611, 2001.
34. Terada, S., and I. Tabata. Effects of acute bouts of running and swimming exercise on PGC-1alpha protein expression in rat epitrochlearis and soleus muscle. *Am. J. Physiol. Endocrinol. Metab.* 286:E208–E216, 2004.
35. Thomas, B. M., and A. T. J. Miller. Adaptation to forced exercise in the rat. *Am. J. Physiol.* 193:350–354, 1958.
36. Thorling, E. B., N. O. Jacobsen, and K. Overvad. Effect of exercise on intestinal tumour development in the male Fischer rat after exposure to azoxymethane. *Eur. J. Cancer Prev.* 2:77–82, 1993.
37. Vogelstein, B., E. R. Fearon, S. R. Hamilton, et al. Genetic alterations during colorectal-tumor development. *N. Engl. J. Med.* 319:525–532, 1988.
38. Vogelstein, B., and K. W. Kinzler. The multistep nature of cancer. *Trends Genet.* 9:138–141, 1993.

Available online at www.sciencedirect.com
ScienceDirect
Biochemical and Biophysical Research Communications 358 (2007) 608–614
BBRC
www.elsevier.com/locate/ybbrc

HnRNP A3 binds to and protects mammalian telomeric repeats *in vitro*

Etsuko Tanaka [a], Hirokazu Fukuda [a], Katsuhiko Nakashima [a], Naoto Tsuchiya [a], Hiroyuki Seimiya [b], Hitoshi Nakagama [a,*]

[a] *Biochemistry Division, National Cancer Center Research Institute, Tsukiji 5, Chuo-ku, Tokyo 104-0045, Japan*
[b] *Division of Molecular Biotherapy, Cancer Chemotherapy Center, Japanese Foundation for Cancer Research, Ariake, Koto-ku, Tokyo 135-8550, Japan*

Received 16 April 2007
Available online 4 May 2007

Abstract

The biological function of hnRNP family proteins is widely diverse and involved in pre-mRNA processing, transcriptional regulation, recombination, and telomere maintenance. In the course of our study on the elucidation of biological functions of minisatellite DNA, we isolated several nuclear proteins that bind to the mouse minisatellite Pc-1, which consists of a tandem array of d(GGCAG) repeats, from NIH3T3 cells. One of the minisatellite binding proteins, MNBP-A, which binds to a single-stranded G-rich strand of the Pc-1 repeat, was proven identical to the hnRNP A3. Recombinant hnRNP A3 was demonstrated to bind to the single-stranded telomeric d(TTAGGG) repeat with much higher affinity than the d(GGCAG) repeat. Binding of hnRNP A3 to the single-stranded telomeric repeat protected the repeat from nuclease attack, and inhibited both telomerase reaction and DNA synthesis *in vitro*. These results suggest a possible biological role of hnRNP A3 in the stable maintenance of telomere repeats.

Keywords: Telomere; HnRNP; Telomerase; Telomere binding protein

Heterogeneous nuclear ribonucleoproteins (hnRNPs) were originally isolated as nuclear RNA-binding proteins that form complexes with pre-mRNA, and many of the members are suspected to be involved in pre-mRNA processing, including transport and splicing [1]. Proteins of the family share high homology with each other in their structural domains. Several members of the hnRNP family are thought to play roles in transcriptional regulation, recombination, and telomere maintenance as DNA-binding proteins, in addition to their action as RNA-binding proteins [2,3]. HnRNP A1, A2/B1, C1/C2, D, and E were indeed demonstrated to associate with telomere and/or telomerase [4–8]. Especially, involvement of hnRNP A1 in telomere-length maintenance was strongly suggested based on several observations. For example, short telomeres were observed in hnRNP A1 deficient mouse CB3 cells, and the telomere-length was restored after expressional reconstitution of hnRNP A1 or its shorter derivative, UP1 in cells [4]. Physiological binding of hnRNP A1 to telomerase, telomerase RNA, and telomeres was also observed [4,9,10]. Furthermore, we previously demonstrated hnRNP A1 and UP1 to unfold the quadruplex structure of the telomeric $d(TTAGGG)_4$ repeat *in vitro*, suggesting a promotive effect of hnRNP A1 on telomerase action through its unfolding activity on quadruplex DNA structures [11]. Recently, hnRNP A1 was indicated to stimulate telomerase activity [12]. In addition, hnRNP family proteins described above and any other members of the hnRNP family proteins are thought to play essential roles in telomere maintenance in a similar manner to hnRNP A1. Therefore, hnRNPs associated with telomeres and telomerase could be good targets for regulating telomere-length [13].

In the course of our study on the mouse hypervariable minisatellite (MN) Pc-1, which is composed of d(GGCAG) tandem repeats, we demonstrated that single-stranded $d(GGCAG)_n$ folds into an intramolecular quadruplex structure under physiological-like conditions and the structure blocks *in vitro* DNA synthesis [14]. The presence of the

* Corresponding author. Fax: +81 33542 2530.
E-mail address: hnakagam@gan2.res.ncc.go.jp (H. Nakagama).

0006-291X/$ - see front matter © 2007 Published by Elsevier Inc.
doi:10.1016/j.bbrc.2007.04.177

characteristic quadruplex structure could therefore be responsible for the hypermutable feature of Pc-1 and other MNs with similar repetitive units. In addition, we have isolated six MN Pc-1 binding proteins (MNBPs) from nuclear extracts of NIH3T3 cells [15]. Two of them, MNBP-A and MNBP-B, bind to the G-rich strand of Pc-1 repeats. MNBP-B was proven identical to UP1, a proteolytic product of hnRNP A1, and was later demonstrated to unfold quadruplex structures formed in G-rich strands of Pc-1 d(GGCAG) repeats and telomeric d(TTAGGG) repeats [11].

In the present study, we document isolation of cDNA clones encoding another MNBP bound to the G-rich strand of Pc-1, MNBP-A, and characterization of a recombinant MNBP-A protein. Sequences of proteolytic peptides of purified MNBP-A were determined and cDNA clones were subsequently isolated. MNBP-A was revealed to be identical to the 39-kDa hnRNP A3. HnRNP A3 has been reported to have a role in cytoplasmic trafficking of RNA in oligodendrocytes [16], but has otherwise been described only at the cDNA level without biochemical and cell biological analysis [17]. DNA-binding specificity and *in vitro* effects of hnRNP A3 on telomeric d(TTAGGG) repeats were here analyzed to cast light on its biological roles.

Materials and methods

Oligonucleotides and plasmids. All synthetic oligonucleotides were purified by reverse-phase cartridge or HPLC chromatography (Sawady Tech. Co., Invitrogen Co., and Grainer Japan Co.). The names and nucleotide sequences of oligonucleotides for EMSA as detailed below, are as follows: pG8, $d(GGCAG)_8$; pG6, $d(GGCAG)_6$; pCGG10, $d(CGG)_{10}$; pTEL5, $d(TTAGGG)_5$; $pTEL5_{6C}$, $d(TTAGGC)_5$; $pTEL5_{2C}$, $d(TCAGGG)_5$; $pTEL5_{3G}$, $d(TTGGGG)_5$; $pG5_{TEL}$, $d(GTTAGG)_5$; Poly-dT, $d(T)_{30}$. poly(dI–dC)/poly(dI–dC) and poly$(dT)_{16}$ were purchased from Amersham Pharmacia Biotech. pSubTEL12: $d(TTAGGG)_{12}$TCTAGT ACTGGCCGTCGTTTTACAACGTCG and its 3′-complementary 24 mer sequence pM13-20 were used for primer extension experiments. pSub15: $d(CAGGG)_{15}$TCTAGTACTGGCCGTCGTTTTACAACGT CG and SubCGG16: dCGACTCTAGA$(CGG)_{16}$TGACTCTAGTA CTGGCCGTCGTTTTACAACGTCG were also used for templates of primer extension.

cDNA cloning for MNBP-A. MNBPs were purified from NIH3T3 cells as described previously [15], and partial polypeptide-sequences were determined by Edman degradation under contract by APRO Science Co. Ltd. (Naruto, Japan). cDNA fragments for the MNBP-A were amplified with a set of degenerated primers, 5′-GTNGARGARGAYGCNATG-3′ and 5′-YTTRTCNACNGTRTCRTCRTG-3′, using cDNAs from NIH3T3 cells as templates. To isolate a full-length MNBP-A cDNA, an NIH3T3 cDNA library in Lambda ZAP II (Stratagene) was screened by plaque hybridization using the partial cDNA fragment described above as a probe. Plasmid pBSA was constructed by cloning the full-length cDNA of MNBP-A into the SacII/HindIII site of the pBluescript II KS vector (Stratagene). Detailed procedures were as described previously [15,18].

Construction of expression vector of recombinant hnRNP A3. To construct an expression vector for the GST-hnRNP A3 fusion protein, an EcoRI fragment of hnRNP A3 cDNA, prepared from pBSA, was inserted into the EcoRI site of the pGEX6P-3 vector (Amersham Pharmacia). The GST fusion protein of hnRNP A3 was expressed in *Escherichia coli* (*E. coli*) and purified, as described previously [19].

EMSA. Electrophoretic mobility-shift assay (EMSA) and analyses of oligonucleotide competition using EMSA were performed as detailed earlier [15] using ^{32}P-labeled oligonucleotides (final conc. 2 nM) applied as a probe with some modifications. After the binding reaction, UV cross-linking was carried out (500 mJ/cm^2). The samples were incubated at 95 °C for 5 min in the presence of SDS-sample buffer [20], and then electrophoresed on 10% SDS–polyacrylamide gel.

In vitro DNA synthesis assay. A primer extension reaction was performed as described previously [21] with some modifications. A mixture of the pSub15, pSubTEL12, or pSubCGG16 with the pM13-20 primer, which was labeled with ^{32}P at the 5′-end (final 100 nM each) in TE buffer containing 150 mM KCl, was heated at 95 °C for 5 min and then at 72 °C for 5 min, followed by gradual cooling, and incubated at 37 °C for 3 h. An aliquot of 1 μl of this primer-annealed template was mixed with 1.5 μl of 5× *Polα* buffer [250 mM Tris–HCl (pH 7.5), 10 mM DTT, 25 mM $MgCl_2$, 1.25 mg/ml BSA], 1 μl of dNTPs mixture (50 μM each) and 2.5 μl of Milli-Q water. After adding 1 μl of the GST-hnRNP A3 (at the final concentrations indicated in the Legend), the mixture was incubated at 37 °C for 30 min, and then the primer extension reaction was carried out at 37 °C for 30 min by the addition of 1 μl of *Polα* DNA polymerase (0.2 U, Chimerx). The concentrations of *Polα* DNA polymerase, the primer-annealed template, and dNTPs were 26.6 U/ml, 13.3 nM, and 6.7 μM, respectively. Only for the reaction using pSubCGG16 as a template, the concentration of dNTPs was reduced to one-fifth (final 1.3 μM each).

Protection of telomeric repeat by hnRNP A3 from nuclease digestion. DNase protection assay was performed as follows. One microliter of ^{32}P-labeled oligonucleotide at the 5′-end (final 4.8 nM) and 1 μl of GST-hnRNP A3 were added into 40 μl of a reaction buffer (40 mM Tris–HCl [pH 8.0], 10 mM $MgSO_4$, 1 mM $CaCl_2$), and incubated at 25 °C for 10 min. After addition of DNase I (5 U, Takara Bio Inc.) or micrococcal nuclease (0.5 U, Takara Bio Inc.), the mixture was incubated at 37 °C for 10 min. The reaction was stopped by the addition of 5 μl of 0.5 M EDTA, and DNA was purified by phenol–chloroform extraction and ethanol precipitation. The DNA samples were electrophoresed on 10%-polyacrylamide gel containing 8 M urea.

Results and discussion

cDNA cloning for mouse hnRNP A3

A 30-kDa minisatellite Pc-1 binding protein, MNBP-A, which was demonstrated to bind to pG8: $d(GGCAG)_8$, representing the G-rich strand of Pc-1, was purified from the NIH3T3 cells as described previously [15], and digested with lysyl endopeptidase in a gel. Amino acid sequences of four peak-fractions of the proteolytic peptide fragments separated by reverse-phase HPLC were determined (Table 1). Only one partial cDNA fragment for MNBP-A was amplified with a set of degenerated primers, 5′-GTNGARGARGAYGCNATG-3′ and 5′-YTTRTCNA CNGTRTCRTCRTG-3′, designed from the peptide-sequences of fragments 1 and 2, as described in Materials and methods. Amplified fragments were subcloned into a pCRII vector, and sequenced. The amino acid sequence deduced from the partial cDNA fragment contained the same sequence as fragments 3 and 4. Therefore, we

Table 1
Amino acid sequences of proteolytic peptides of MNBP-A

Fragment	Amino acid sequence
1	RSRGFGFVTY(A/S)XV(E/L)EVDAAMXARPXX
2	RGFAFVTFDDHDTVDK
3	RAVSREDSVK
4	IETIEVMEDRQSGK

concluded that this fragment is really the partial cDNA for MNBP-A. Using this cDNA fragment as a probe, one cDNA clone containing the cDNA sequence was isolated from the NIH3T3 cDNA library. Its deduced amino acid sequence showed 99.2% identity to that of human heterogeneous nuclear ribonucleoprotein A3 (hnRNP A3). All the sequences of proteolytic peptide fragments of MNBP-A were coincident with the amino acid sequence deduced from the cDNA sequences, although the sequence of fragment 1 contained 4X (not determined) residues. Furthermore, only three amino acid residues were substituted from the corresponding sequences of human hnRNP A3. Therefore, we hereafter refer to MNBP-A as mouse hnRNP A3. The nucleotide sequence of cDNA for mouse hnRNP A3 was submitted to DDBJ (Accession No. AB201711).

In vitro binding of hnRNP A3 to telomeric repeat with the highest affinity

A recombinant protein of hnRNP A3 expressed in *E. coli* as a GST fusion protein was purified (Fig. 1A). GST-hnRNP A3 protein bound to the single-stranded oligonucleotide d(GGCAG)$_6$ and d(GTTAGG)$_5$ with high affinities (Fig. 1B). On the other hand, binding of GST-hnRNP A3 to oligonucleotide d(CGG)$_{10}$ was hardly detectable by EMSA (Fig. 1B), although the DNA–protein complex was observed by longer exposure (data not shown). Binding of GST protein alone to these oligonucleotides could not be detected by EMSA (data not show). In order to clarify the sequence-specificity for DNA binding of hnRNP A3, we performed an oligonucleotide competition assay using EMSA (Fig. 2). GST-hnRNP A3 bound to d(GTTAGG)$_5$ with the highest affinity, corresponding to our previous results regarding binding properties of MNBP-A/hnRNP A3 purified from NIH3T3 cells [15]. The affinity of hnRNP A3 to d(TTAGGG)$_5$ was weaker than to d(GTTAGG)$_5$, although the difference in sequence between the two oligonucleotides is subtle. Base substitutions into the second or third nucleotide of the repeat unit, d(TTAGGG), reduced the affinity of hnRNP A3 to each oligonucleotide, suggesting that the intervening sequence of d(TTA) is also important for determining the binding specificity of hnRNP A3. The affinity of hnRNP A3 for oligo RNA r(GUUAGG)$_5$ was about the same as that for corresponding oligo DNA d(GTTAGG)$_5$ (data not shown).

We next monitored both association and dissociation processes in real time using an SPR Biosensor system (Biacore). SPR biosensor analysis also indicated a high affinity of hnRNP A3 to the telomeric d(TTAGGG) repeat (Supplementary Fig. 1A). The value of K_D (equilibrium dissociation constant) for GST-hnRNP A3 to d(TTAGGG)$_5$ was estimated to be 2.6 nM from the sensorgrams. The sensorgrams in the dissociation phase indicated that the complex between GST-hnRNP A3 and d(TTAGGG)$_5$ was considerably stable (Supplementary Fig. 1A). The K_D value to d(GGCAG)$_6$ was 5.2 nM, indicating that the affinity of the protein to d(GGCAG)$_6$ was half of that to d(TTAGGG)$_5$ (Supplementary Fig. 1B). On the other

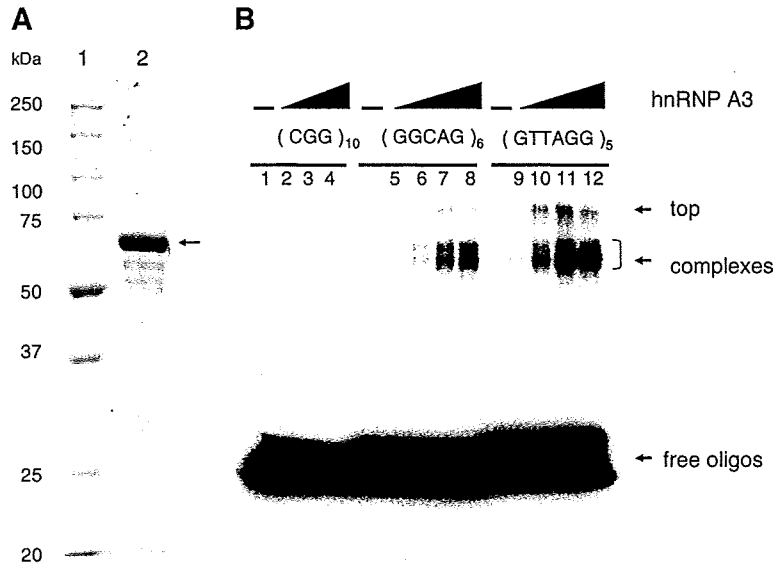

Fig. 1. Purification of GST-hnRNP A3 protein and sequence-specificity of its DNA binding. (A) SDS–PAGE image of purified GST-hnRNP A3 protein stained with Coomassie brilliant blue. The protein (lane 2) is indicated by an arrow, and molecular weights of each marker protein (lane 1) are shown on the left side of the panel. (B) Electrophoretic mobility-shift assay (EMSA) of GST-hnRNP A3 to d(CGG)$_{10}$, d(GGCAG)$_6$, and d(GTTAGG)$_5$. The final concentration of labeled probes, d(CGG)$_{10}$ (lanes 1–4), d(GGCAG)$_6$ (lanes 5–8), and d(GTTAGG)$_5$ (lanes 9–12) was 20 nM. Final concentrations of GST-hnRNP A3 were 2.4 nM (lanes 2, 6, and 10), 12 nM (lanes 3, 7, and 11), and 60 nM (lanes 4, 8, and 12). GST (final 300 nM) was used as a negative control (lanes 1, 5, and 9).

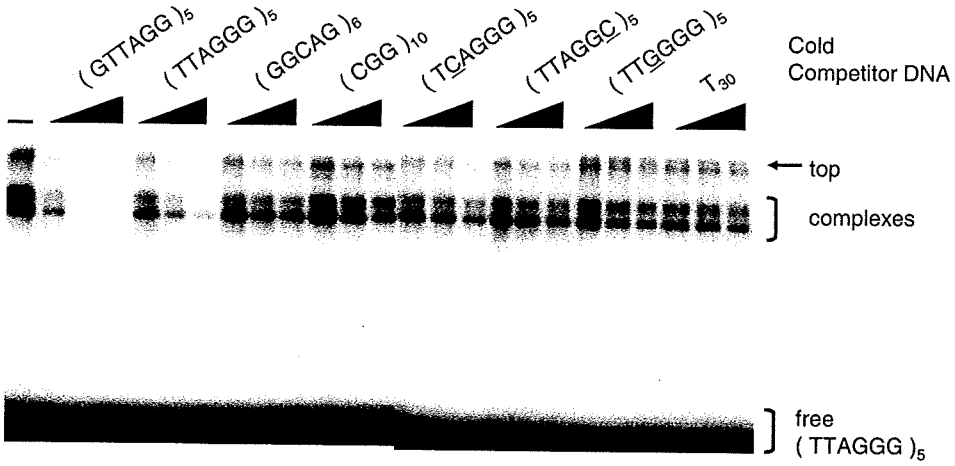

Fig. 2. HnRNP A3 binds to d(TTAGGG)$_n$ telomeric repeat with a high affinity. EMSA of GST-hnRNP A3 to labeled d(TTAGGG)$_5$ in the presence of each cold competitor oligonucleotide (indicated above the panel). Final concentrations of the labeled probe and GST-hnRNP A3 were 20 and 60 nM, respectively. The lane at the left end was a control without cold competitor. Each competitor oligonucleotide was added at final concentrations of 20 nM, 200 nM, and 2 μM (from left to right in each triplicate lanes).

hand, the complex between GST-hnRNP A3 and d(CGG)$_{10}$ was unstable (Supplementary Fig. 1C). The K_D value to d(CGG)$_{10}$ was 0.24 μM.

Recombinant purified hnRNP A3 was demonstrated above to bind *in vitro* to a single-stranded G-rich telomeric repeat with a high affinity. Several other members of the hnRNP family, hnRNP A1, A2/B1, D, and E, CBF-A, uqTBP25, and Gbp1p of Chlamydomonas, were reported to bind to the ss G-strand of a telomeric repeat *in vitro* and supposed to associate with the G-strand overhang of telomeres *in vivo* [5,6,9,13,22–24]. The affinity of hnRNP A3 to the d(TTAGGG) repeat is stronger than or similar to those of the other hnRNPs mentioned above. It is, therefore, highly possible that hnRNP A3 associates with telomeres *in vivo* and plays a role in telomere maintenance. The affinity of hnRNP A3 to d(TTAGGG)$_5$ was weaker than that to d(GTTAGG)$_5$. The difference of higher-order structure formations between d(TTAGGG)$_5$ and d(GTTAGG)$_5$, depending on the number of d(GGG) stretches within the repeats, may have a substantial influence on the binding affinity between the two oligonucleotides.

In vitro effect of hnRNP A3 on nuclease digestion and DNA synthesis on telomeric repeat sequences

In order to elucidate the biological function of hnRNP A3, we first examined effects of hnRNP A3 on nuclease digestion of the telomeric repeats. DNase I-digested naked single-stranded oligonucleotide d(TTAGGG)$_{10}$ almost completely (Fig. 3, lane 1). The presence of GST alone in the mixture of DNase I and d(TTAGGG)$_{10}$ did not show any effect on the digestion (Fig. 3, lane 2). In contrast, addition of GST-hnRNP A3 inhibited the digestion of d(TTAGGG)$_{10}$ with DNase I in a dose-dependent manner (Fig. 3, lanes 3–7). Almost all of the telomeric repeats were perfectly protected from DNase I at a high concentration

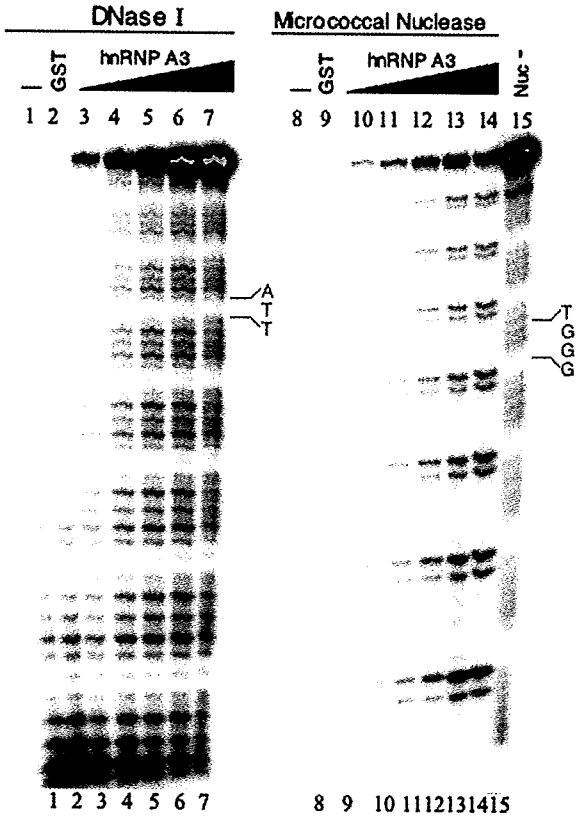

Fig. 3. Protection of telomeric d(TTAGGG) repeats from nuclease digestion by the binding of hnRNP A3. Labeled oligonucleotide d(TTAGGG)$_{10}$ was digested with DNase I (lanes 1–7) or micrococcal nuclease (lanes 8–14) in the presence of GST-hnRNP A3. Lane 15, lanes 1 and 8, and lanes 2 and 9 were controls without nucleases, without either GST-hnRNP A3 or GST, with addition of GST in place of GST-hnRNP A3, respectively. Concentrations of GST-hnRNP A3 were 8.8 nM (lanes 3 and 10), 18 nM (lanes 4 and 11), 35 nM (lanes 5 and 12), 70 nM (lanes 6 and 13), and 140 nM (lanes 7 and 14). Protected sequence from each nuclease is shown on the right side.

of GST-hnRNP A3 (Fig. 3, lanes 6 and 7). Cyclic patterns of DNase I-digested d(TTAGGG)$_{10}$ indicated that every (TTA) stretch in the telomeric repeat units was protected by the binding of GST-hnRNP A3. This suggests that each RNA-recognition motif (RRM) of the two RRMs in a hnRNP A3 molecule recognize 1 U of telomeric repeat, consistent with the study about the crystal structure of hnRNP A1 with telomeric repeats [25].

Binding of GST-hnRNP A3 also protected d(TTAGGG)$_{10}$ from digestion with micrococcal nuclease in a dose-dependent manner (Fig. 3, lanes 10–14), and a complete protection was observed at higher concentrations. It is interesting to note that the digestion patterns with micrococcal nuclease were drastically different from those with DNase I. Every (GGGT) sequence in the telomeric unit was protected from the attack of micrococcal nuclease by the binding of GST-hnRNP A3 (Fig. 3, lanes 10–14). This difference was unexpected, but probably came from the difference of the accessibility of the two nucleases to the hnRNP A3-d(TTAGGG)$_{10}$ complex.

We next examined effects of hnRNP A3 on DNA synthesis on the telomeric repeats. HnRNP A3 inhibited the DNA synthesis on d(TTAGGG)$_{12}$ repeat in a dose-dependent manner (Fig. 4A). Since hnRNP A3 binds strongly to d(TTAGGG)$_n$ and the complex is remarkably stable (Supplementary Fig. 1A), hnRNP A3 is likely to block the procession of DNA polymerase. Similar results were obtained with the d(CAGGG)$_n$ repeat (Fig. 4B). In contrast, hnRNP A3 abrogated the arrest of DNA synthesis on the template with d(CGG)$_{16}$ repeat to some extent at only higher concentrations (Fig. 4C).

Binding of hnRNP A3 protects the G-strand of telomeric repeats from nuclease attack, and DNA polymerase (Figs. 3 and 4). The result suggests the possibility that hnRNP A3 may constitute a capping structure to protect the 3′-overhang of telomeres together with other proteins including hnRNPs. Telomeres are proposed to form a t-loop structure that sequesters chromosomal ends by invasion of the telomeric 3′-overhang into the telomeric duplex [26]. It is unknown whether hnRNP A3 can associate with the telomeric 3′-overhang forming the t-loop structure *in vivo*. However, the binding of hnRNP A3 to the 3′-overhang of telomeres may play an important role in preventing access to a variety of enzymes, including nucleases and telomerase, at some point during the cell cycle.

Possible involvement of hnRNP A3 in telomere maintenance

HnRNP A1 was demonstrated *in vitro* to unfold the intramolecular quadruplex structure of telomeric repeats [11] and to stimulate telomerase activity [12]. Physical

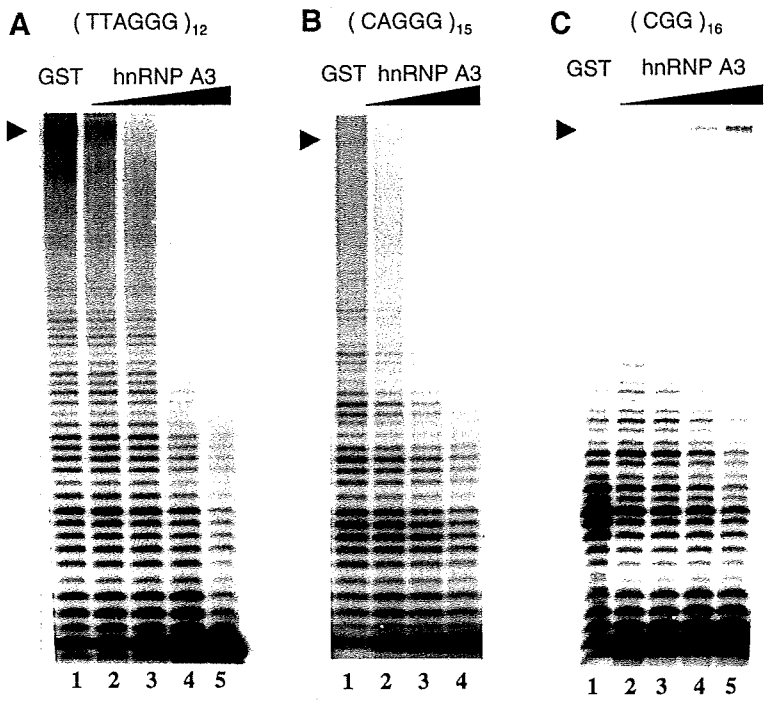

Fig. 4. Effect of GST-hnRNP A3 on *in vitro* DNA synthesis of G-rich repeats. Results of polyacrylamide gel electrophoresis indicating the primer extension reaction with GST or GST-hnRNP A3, using the single-stranded oligonucleotide templates carrying d(TTAGGG)$_{12}$ (A), d(CAGGG)$_{15}$ (B), and d(CGG)$_{16}$ (C). The concentrations of GST-hnRNP A3 were 50 nM (lanes 2 and 7), 100 nM (lanes 3 and 8), 200 nM (lanes 4 and 9), 400 nM (lane 5), 500 nM (lane 11), 1 μM (lane 12), 2 μM (lane 13), 14 μM (lane 14), respectively. Concentration of GST was 400 nM (lanes 1, 6, and 10). Arrow heads indicate the positions of the full-length synthesized products. Note that the full-length products for the template containing d(CGG)$_{16}$ were increased depending on the amount of hnRNP A3.

interaction of hnRNP A1 with telomeric DNA and human telomerase RNA was also reported [10]. Loss of hnRNP A1 in mouse cells correlated with short telomeres and expression of hnRNP A1 or UP1 restored the normal length of telomeric repeats [4]. Taking these data together, hnRNP A1 is thought to be involved in telomere maintenance by stimulating telomerase activity through its ability to modulate a tertial structure of the telomere end [12,13,27]. HnRNP A2/B1, C1/C2, D, and E were demonstrated to associate with telomeres or/and telomerase [5–8] and suggested to play some roles in telomere metabolism. These hnRNPs were considered as multi-functional proteins involved in both mRNA processing and DNA metabolisms, including telomere- and transcriptional regulation. As compared with those hnRNPs, the functions of hnRNP A3 are largely unknown although there are only two reports describing its functions. One reported that it is a component of the 40S hnRNP complex [17], and the other suggested that it has a role in cytoplasmic trafficking of RNA [16]. In the present study, hnRNP A3 was demonstrated to bind to the single-stranded telomeric d(TTAGGG) repeat with a remarkably high affinity. Protection of telomeric sequences from nucleases by its binding was also indicated *in vitro*. It is highly possible that the protein plays a role in telomere elongation as well as hnRNP A1, or other processes in telomere regulation.

Acknowledgments

This work was supported by a Grant-in-Aid for Cancer Research from the Ministry of Health, Labour, and Welfare of Japan, and Grants-in-Aid for Scientific Research from the Ministry of Education, Culture, Sports, Science, and Technology of Japan. H.F. was supported by a Research Grant of the Princess Takamatsu Cancer Research Fund, and the Senri Life Science Foundation.

Appendix A. Supplementary data

Supplementary data associated with this article can be found, in the online version, at doi:10.1016/j.bbrc.2007.04.177.

References

[1] G. Dreyfuss, M.J. Matunis, S. PionlRoma, C.G. Burd, HnRNP proteins and the biogenesis of mRNA, Annu. Rev. Biochem. 269 (1993) 289–321.
[2] A.M. Krecic, M.S. Swanson, HnRNP complexes: composition, structure, and function, Curr. Opin. Cell Biol. 11 (1999) 363–371.
[3] M. Ladomery, Multifunctional proteins suggest connections between transcriptional and post-transcriptional processes, Bioessays 19 (1997) 903–909.
[4] H. LaBranche, S. Dupuis, Y. Ben-David, M.R. Bani, R.J. Wellinger, B. Chabot, Telomere elongation by hnRNP A1 and a derivative that interacts with telomeric repeats and telomerase, Nat. Genet. 19 (1998) 199–202.
[5] S.J. McKay, H. Cooke, HnRNP A2/B1 binds specifically to single stranded vertebrate telomeric repeat TTAGGGn, Nucleic Acids Res. 20 (1992) 6461–6464.
[6] F. Ishikawa, M.J. Matunis, G. Dreyfuss, T.R. Cech, Nuclear proteins that bind the pre mRNA 3′ splice site sequence r(UUAG/G) and the human telomeric DNA sequence d(TTAGGG)$_n$, Mol. Cell. Biol. 13 (1993) 4301–4310.
[7] A. Eversole, N. Maizels, In vitro properties of the conserved mammalian protein hnRNP D suggest a role in telomere maintenance, Mol. Cell Biol. 20 (2000) 5425–5432.
[8] L.P. Ford, J.M. Suh, W.E. Wright, J.W. Shay, Heterogeneous nuclear ribonucleoproteins C1 and C2 associate with the RNA component of human telomerase, Mol. Cell Biol. 20 (2000) 9084–9091.
[9] F. Dallaire, S. Dupuis, S. Fiset, B. Chabot, Heterogeneous nuclear ribonucleoprotein A1 and UP1 protect mammalian telomeric repeats and modulate telomere replication in vitro, J. Biol. Chem. 275 (2000) 14509–14516.
[10] S. Fiset, B. Chabot, HnRNP A1 may interact simultaneously with telomeric DNA and the human telomerase RNA in vitro, Nucleic Acids Res. 29 (2001) 2268–2275.
[11] H. Fukuda, M. Katahira, N. Tsuchiya, Y. Enokizono, T. Sugimura, M. Nagao, H. Nakagama, Unfolding of quadruplex structure in the G-rich strand of the minisatellite repeat by the binding protein UP1, Proc. Natl. Acad. Sci. USA 99 (2002) 12685–12690.
[12] Q.-S. Zhang, L. Manche, R.-M. Xu, A.R. Krainer, HnRNP A1 associates with telomere ends and stimulates telomerase activity, RNA 12 (2006) 1116–1128.
[13] L.P. Ford, W.E. Wright, J.W. Shay, A model for heterogeneous nuclear ribonucleoproteins in telomere and telomerase regulation, Oncogene 21 (2002) 580–583.
[14] M. Katahira, H. Fukuda, H. Kawasumi, T. Sugimura, H. Nakagama, M. Nagao, Intramolecular quadruplex formation of the G-rich strand of the mouse hypervariable minisatellite Pc-1, Biochem. Biophys. Res. Commun. 264 (1999) 327–333.
[15] H. Fukuda, T. Sugimura, M. Nagao, H. Nakagama, Detection and isolation of minisatellite Pc-1 binding proteins, Biochim. Biophys. Acta 1528 (2001) 152–158.
[16] A.S. Ma, K. Moran-Jones, J. Shan, T.P. Munro, M.J. Snee, K.S. Hoek, R. Smith, Heterogeneous nuclear ribonucleoprotein A3, a novel RNA trafficking response element-binding protein, J. Biol. Chem. 277 (2002) 18010–18020.
[17] A. Plomaritoglou, T. Choi-Papadopoulou, A. Guialis, Molecular characterization of a murine, major A/B type hnRNP protein: mBx, Biochim. Biophys. Acta 1490 (2000) 54–62.
[18] N. Tsuchiya, H. Fukuda, T. Sugimura, M. Nagao, H. Nakagama, LRP130, a protein containing nine pentatricopeptide repeat motifs, interacts with a single-stranded cytosine-rich sequence of mouse hypervariable minisatellite Pc-1, Eur. J. Biochem. 269 (2002) 2927–2933.
[19] H. Fukuda, H. Shima, R.F. Vesonder, H. Tokuda, H. Nishino, S. Katoh, S. Tamura, T. Sugimura, M. Nagao, Inhibition of protein serine/threonine phosphatases by fumonisin B1, a mycotoxin, Biochem. Biophys. Res. Commun. 220 (1996) 160–165.
[20] U. Laemmli, Cleavage of structural proteins during the assembly of the head of bacteriophage T4, Nature 227 (1970) 680–685.
[21] H. Fukuda, M. Katahira, E. Tanaka, Y. Enokizono, N. Tsuchiya, K. Higuchi, M. Nagao, H. Nakagama, Unfolding of higher DNA structures formed by the d(CGG) triplet repeat by UP1 protein, Genes Cells 10 (2005) 953–962.
[22] G. Sarig, P. Weisman-Shomer, R. Erlitzki, M. Fry, Purification and characterization of qTBP42, a new single-stranded and quadruplex telomeric DNA-binding protein from rat hepatocytes, J. Biol. Chem. 272 (1997) 4474–4482.
[23] R. Erlitzki, M. Fry, Sequence-specific binding protein of single-stranded and unimolecular quadruplex telomeric DNA from rat hepatocytes, J. Biol. Chem. 272 (1997) 15881–15890.

[24] S.D. Johnston, J.E. Lew, J. Berman, Gbp1p, a protein with RNA recognition motifs, binds single-stranded telomeric DNA and changes its binding specificity upon dimerization, Mol. Cell Biol. 19 (1999) 923–933.
[25] J. Ding, M.K. Hayashi, Y. Zhang, L. Manche, A.R. Krainer, R.M. Xu, Crystal structure of the two-RRM domain of hnRNP A1 (UP1) complexed with single-stranded telomeric DNA, Genes Dev. 13 (1999) 1102–1115.
[26] J.D. Griffith, L. Comeau, S. Rosenfield, R.M. Stansel, A. Bianchi, H. Moss, T. de Lange, Mammalian telomeres end in a large duplex loop, Cell 97 (1999) 3–14.
[27] H. Nakagama, K. Higuchi, E. Tanaka, N. Tsuchiya, K. Nakashima, M. Katahira, H. Fukuda, Molecular mechanisms for maintenance of G-rich short tandem repeats capable of adopting G4 DNA structures, Mutat. Res. 598 (2006) 120–131.

Available online at www.sciencedirect.com
ScienceDirect
Biochemical and Biophysical Research Communications 357 (2007) 828–833
BBRC
www.elsevier.com/locate/ybbrc

Identification of dermcidin in human gestational tissue and characterization of its proteolytic activity

Jin-Pyo Lee Motoyama [a,*], Hoon Kim-Motoyama [b], Phyo Kim [c], Hitoshi Nakagama [d], Kiyoshi Miyagawa [e], Kenji Suzuki [a,f]

[a] *Department of Obstetrics and Gynecology, Keiyu Hospital, Kanagawa, Japan*
[b] *Motoyama Medical Clinic, Tokyo, Japan*
[c] *Department of Neurosurgery, Dokkyo Medical University, Tochigi, Japan*
[d] *Biochemistry Division, National Cancer Center Research Institute, Tokyo, Japan*
[e] *Section of Radiation Biology, Graduate School of Medicine, The University of Tokyo, Tokyo, Japan*
[f] *Department of Obstetrics and Gynecology, School of Medicine, Keio University, Tokyo, Japan*

Received 24 February 2007
Available online 28 March 2007

Abstract

Dermcidin (DCD) is a gene for an antimicrobial peptide DCD-1 in human sweat glands. It has become evident that the gene products of DCD exhibit a wide range of biological functions. In addition to its antimicrobial function, it is reported to be a neuronal survival factor, a putative oncogene in breast cancer and a proteolysis-inducing factor (PIF) that induces skeletal muscle proteolysis to cause cancer cachexia. Here we identified DCD in human placental tissue and determined its previously uncharacterized proteolytic activity. We also show that recombinant DCD induced an invasive phenotype in a human choriocarcinoma cell line JAR in vitro. This work suggests that DCD might participate in the regulation of placental function by means of modulating the proteolytic cascades on the trophoblastic cell surface, and might be involved in the pathophysiology of pregnancy-related disorders, as well as cancer and neuronal diseases.

Keywords: DCD; Placenta; Proteolysis; Protease; Invasion; Trophoblast

Proteases regulate a wide range of cellular functions by processing bioactive molecules. They control important biological processes such as DNA replication, cell-cycle progression, proliferation, apoptosis, differentiation/dedifferentiation, angiogenesis, migration and invasion, immunity, and tissue remodelling [1]. In cellular microenvironments, most proteolytic activities are confined to the immediate pericellular space. Modification of cell surface and extracellular matrix (ECM) molecules by proteolysis regulates extracellular signal transduction and cell behavior [2,3].

Dermcidin (DCD) was originally identified as a gene for an antimicrobial peptide DCD-1 in human sweat glands [4]. It has become evident that the gene products of DCD have not only antimicrobial function, but a wide range of biological functions. N-terminal 30 amino acid peptide of DCD, known as either survival-promoting peptide, diffusible survival evasion peptide (DSEP) or Y-P 30 [5,6], which was isolated from oxidatively stressed neural cell lines, is reported to promote neural cell survival under oxidative conditions. Using serial analysis of gene expression (SAGE) analysis, another group identified DCD as a candidate oncogene of breast cancer [7], hypothesizing that DCD might play a role in tumorigenesis by means of enhancing cell growth and survival in a subset of breast carcinomas. Proteolysis-inducing factor (PIF) was originally identified as a mouse cachectic factor and induces skeletal muscle proteolysis [8,9]. DCD is reported to be a human homologue of mouse PIF, based on the 90% amino

* Corresponding author. Address: Department of Obstetrics and Gynecology, Keiyu Hospital, Kanagawa, Japan.
E-mail address: jplm@pop02.odn.ne.jp (J.-P. Lee Motoyama).

0006-291X/$ - see front matter © 2007 Elsevier Inc. All rights reserved.
doi:10.1016/j.bbrc.2007.03.112